Published in final edited form as:
RSC Adv. 2014 January 1; 4(102): 58762–58768. doi:10.1039/C4RA11225C.

Central C-C Bonding Increases Optical and Chemical Stability of NIR Fluorophores

Hoon Hyun[1,*], **Eric A. Owens**[2,*], **Lakshminarayana Narayana**[2], **Hideyuki Wada**[1], **Julien Gravier**[1], **Kai Bao**[1], **John V. Frangioni**[1,3,4], **Hak Soo Choi**[1,**], and **Maged Henary**[2,**]

[1]Division of Hematology/Oncology, Department of Medicine, Beth Israel Deaconess Medical Center and Harvard Medical School, Boston, MA 02215

[2]Department of Chemistry, Center for Diagnostics and Therapeutics, Georgia State University, Atlanta, GA 3030

[3]Department of Radiology, Beth Israel Deaconess Medical Center and Harvard Medical School, Boston, MA 02215

[4]Curadel, LLC, 377 Plantation Street, Worcester, MA 01605, USA

Abstract

Functional near-infrared (NIR) fluorophores have played a major role in the recent advances in bioimaging. However, the optical and physicochemical stabilities of NIR fluorophores in the biological and physiological environment are still a challenge. Especially, the ether linkage on the *meso* carbon of heptamethine core is fragile when exposed to serum proteins or other amine-rich biomolecules. To solve such a structural limitation, a rigid carbon-carbon bond was installed onto the framework of ether-linked NIR fluorophores through the Suzuki coupling. The robust fluorophores replaced as ZW800-1C and ZW800-3C displayed enhanced optical and chemical stability in various solvents and a 100% warm serum environment (> 99%, 24 h). The biodistribution and clearance of C-C coupled ZW800 compounds were almost identical to the previously developed oxygen-substituted ZW800 compounds. When conjugated with a small molecule ligand, ZW800-1C maintained the identical stable form in warm serum (>98%, 24 h), while ZW800-1A hydrolyzed quickly after 4 h incubation (34%, 24 h).

Keywords

Suzuki-coupling; Near-Infrared Fluorescence; Optical Imaging; Image-Guided Surgery; Signal-to-Background Ratio

**Corresponding Authors: Hak Soo Choi, Ph.D., 330 Brookline Avenue, Room SL-436A, Boston, MA 02215, Office: 617-667-6024; Fax: 617-975-5016, hchoi@bidmc.harvard.edu. Maged Henary, Ph.D., 100 Piedmont Ave. #315, Atlanta, GA 30303, Office: 404-413-5566; Fax: 404-413-5505, mhenary1@gsu.edu.
*These authors contributed equally to this work.

AUTHOR CONTRIBUTIONS

HH, EAO, LN, HW, JG, and KB performed the experiments. HH, EAO, JVF, MH, and HSC reviewed, analyzed, and interpreted the data. HH, EAO, JVF, MH, and HSC wrote the paper. All authors discussed the results and commented on the manuscript.

COMPETING FINANCIAL INTERESTS

John V. Frangioni, M.D., Ph.D.: Dr. Frangioni is currently CEO of Curadel, LLC, which has licensed FLARE imaging systems and contrast agents from the Beth Israel Deaconess Medical Center.

Recent development in bioimaging and theragnostics requires highly stable and functional near-infrared (NIR) fluorophores.[1–4] Particularly, carbocyanine fluorophores composed of polymethine chromophores with an odd number of carbon atoms have been successfully used for biological and intraoperative imaging.[5–16] Since they have large molar absorptivity in the NIR region (650–900 nm), the cyanine fluorophores have diverse utility from NIR laser dyes, fluorescent label DNA sequencing, to immunoassays and binding analyses of biomolecule-fluorophore interactions.[17–20]

We have recently reported the successful development of zwitterionic heptamethine indocyanine fluorophores that have high molecular brightness including both high extinction coefficient and quantum yield in serum protein and rapid renal clearance from the body without nonspecific uptake in major organs.[7–9] Moreover, when the central reactive carboxylate moiety is modified with a targeting ligand, we have observed unprecedented visualization of tumors *in vivo* with almost no background retention.[8] By controlling the physicochemical properties of a contrast agent, the signal-to-background ratio could be maximized for *in vitro* diagnostics as well as *in vivo* imaging. However, decreasing fluorescence arisen from the ether linkage on the heptamethine core of NIR fluorophores in serum was recently disclosed when applying for various purposes by conjugating into proteins, antibodies, and amine-rich polymers such as polylysine. We hypothesized that the central oxygen linking modality to the chromophore could be labile during amide-coupling chemistry and while circulating throughout the blood stream *in vivo*.

To circumvent this molecular shortcoming and observe the potential biological perturbation associated with a new set of fluorophores, in this study, we incorporated a central carbon-carbon (C-C) bond that locks the conformation and increases the chemical robustness of the central linker. The *meso* position substitution of the heptamethine fluorophores has continuously been investigated,[21,22] and it is well known that their essential optical properties including absorption and emission wavelengths, Stokes shift, extinction coefficient, quantum yield, and photostability are directly influenced by the substitution at this position. Therefore, we also performed optical and chemical stability of C-C coupled heptamethine fluorophores *in vitro* as well as their biodistribution and clearance in small and large animals.

Results and Discussion

The synthetic routes to prepare the zwitterionic precursors **1** and **2** have been systemically established by our group in pursuit of ZW800-1A and ZW800-3A as shown in Figure 1A.[7–9] On the intermediate compounds **1** and **2**, the central C-C bonds were installed by a boronic acid functionalized linker *in lieu* of the previously used phenoxy linker through the Suzuki coupling method using tetrakistriphenylphosphine palladium(0) as a catalyst. The advantages of Suzuki coupling over other reactions are availability of common boronic acids, mild reaction conditions using aqueous media, and the less toxic nature than other similar reactions. Boronic acids are less toxic and safer for the environment than organostannane and organozinc compounds. It is easy to remove the inorganic byproducts from reaction mixture. Thus, Suzuki reaction is good enough for the future clinical use of those fluorophores. The **3** (ZW800-1C) and **4** (ZW800-3C) fluorophores were obtained in

reasonable yields (72% and 34%, respectively) and purified by reverse phase column chromatography, because highly pure products are required for the *in vivo* use and accurate measurement of optical properties. The analytical purities of **3** and **4** fluorophores were confirmed by using liquid chromatography-mass spectrometry (LC-MS) that showed > 98% purity according to both the optical absorption detected at 700 nm and the total ion count for the mass spectrometer (Figure 1B). The highly charged molecular character causes several identification peaks to be visible in the mass spectra with the m/z ratio being the highest molecular weight with the lower mass peaks corresponding to higher charges. The LC-MS result indicates that the ultrapure fluorophores could provide reliable optical properties and *in vivo* performances.

Interestingly, ZW800-1C displays H-aggregation in phosphate buffered saline (PBS, pH 7.4) as indicated by the blue-shifted peak compared to the ZW800-3C; when phenomenon was not observed in our previous study of ZW800-1A (Figure 1C). As the concentration of the fluorophore was increased, we observe an absorbance increase for the blue-shifted peak in comparison to the red-shifted peak which is known as the dimerization phenomenon. We assume that the hydrophobic interior of the C-C coupled compound **3** aligns in the intermolecular aggregation due to the highly charged character pointing toward the hydrophilic solvent; however, ZW800-1A has two characteristics that prevent this dimerization phenomenon, the rotary ability and polarity of the *meso*-phenoxy moiety. Additionally, ZW800-1C exhibited a decrease of dimerization in fetal bovine serum (FBS, pH 7.4) supplemented with 50 mM HEPES (4-(2-hydroxyethyl)-1-piperazineethanesulfonic acid) compared to the absorption spectrum in PBS buffer, because the blue-shifted peak was significantly lower (Figure 1C). Fortunately, this indicates that serum proteins prevent the dimerization of ZW800-1C, so that ZW800-1C could behave like ZW800-1A *in vivo* without nonspecific tissue/organ uptake due to the micro-aggregations. They show reasonably high molar extinction coefficients with large stokes shift values in various solvents and effective quantum yield and overall molecular brightness in FBS reflecting their solubility that more hydrophilic ZW800-1C has higher optical absorption than ZW800-3C in an aqueous solution (Figure 1D and 1E and Table S1 in Supplementary Information).

The physicochemical properties of C-C bonded fluorophores were compared with oxygen-substituted derivatives in Figure 2. Although the *in silico* physicochemical properties calculated by JChem Plugin (ChemAxon) were almost identical, C-C coupled compounds showed extremely high serum stability (> 99%) up to 24 h. On the other hand, the previous fluorophores containing the phenoxy linker were degraded by serum proteins, and finally broke down to chemical compounds with blue-shifted absorbance properties (~50% at 24 h). The electron donating capabilities of the phenyl ring helps to reduce the electrophilicity of the polymethine bridge thus increasing the chemical stability; whereas, the oxygen-based linking substituent has electron withdrawing characteristics which corresponds to a more highly electron deficient core of the dye and lowers the overall stability. The hydrophobicity between **3** and **4** fluorophores (LogD at pH 7.4: −2.80 and −1.25) supports the different retention times of them shown in the LC-MS analysis. It is related to the total polar surface area (TPSA) of **3** and **4** fluorophores calculated as 157.95 Å and 43.44 Å, respectively. The

hydrophobicity and polarity of fluorophores are very important factors related to *in vivo* behavior because it makes potentially different biodistribution. We previously reported the effect of hydrophobicity and polarity in terms of the body excretion of fluorophore.[7] The study proves that the fluorophore having negatively charged and/or highly hydrophilic properties excretes through renal clearance, while the positively charged and/or hydrophobic fluorophore shows hepatic clearance from liver to duodenum. Pharmacokinetically it is known that molecules with a polar surface area of greater than 140 Å tend to be poor at permeating cell membranes.

In order to determine *in vivo* performance, the C-C bonded fluorophores were injected intravenously into 25 g CD-1 mice and 250 g SD rats (Figure 3A–B). ZW800-1C showed exactly the same behavior as ZW800-1A in rodent resulting in a rapid renal excretion (> 80%) at 4 h post-injection, non-organ/tissue uptake, and ultralow background. Also, ZW800-3C has the identically same biodistribution and clearance with previously reported ZW800-3A.[7] About 25% of injected molecules excreted to urine and the rest went through the hepatobiliary clearance route. The *in vivo* results of ZW800-1C and ZW800-3C prove that the chemical modification on the *meso*-position does not affect the *in vivo* performances.

To confirm the biodistribution pattern in large animals, we injected 5 μmol of ZW800-1C and ZW800-3C in 35 kg Yorkshire pigs. As shown in Figure 3C, the zwitterionic compound ZW800-1C was rapidly cleared through the kidney filtration with nearly negligible liver uptake. The elevated kidney signals decreased significantly in accordance with urinary excretion over 4 h (data not shown). Also, the compound ZW800-3C without sulfonate-groups showed nonspecific uptake in skin (~20%), kidneys (~9%), and liver (~7%) at 4 h post-intravenous injection, which is mostly associated with increased hydrophobicity and serum protein interaction.[7] Thus, they showed similar *in vivo* performances in small and large animals, and are convinced that C-C bonded structures of them maintain their original behaviors as well as make improvement of stability in biological conditions.

In our previous study, ZW800-1A showed excellent *in vivo* performance such as rapid renal clearance, ultralow background, and high molecular brightness.[7–9] Furthermore, ZW800-1A could be applied for efficient tumor targeting when conjugated with a tumor-specific ligand such as cyclic RGD peptides, which proved outstanding tumor targeting with minimal nonspecific binding compared to conventional fluorophores including IRDye800CW and Cy5.5.[7] However, the only drawback of ZW800-1A includes the long-term instability in base- and protein-containing environments, because the labile ether linkage of ZW800-1A is easily hydrolyzed in base conditions and attacked by amine-bearing molecules during conjugation reaction resulting in the formation of undesirable byproducts (Figure 4A). This indicates that the structure changes of ZW800-1A on the *meso*-position in both nitrogen substitution and aldehyde formation can lead to the blue-shift of the absorbance peak followed by the loss of fluorescence. Initially, our focus was only on the short-term stability of ZW800-1A and ZW800-3A in warm serum because of their potential usage as blood pooling agents.[7] However, when they were conjugated to proteins and polymers, both compounds showed unexpected degradation during the long-term storage over 24 h. Thus, we investigated their time-dependent stabilities using ZW800-1A and ZW800-1C when

conjugated with various amine-bearing molecules such as cRGDyK peptide, bovine serum albumin (BSA), antibody, and poly-ε-lysine. As shown in Figure 4B, ZW800-1C conjugates show high photostability in warm serum (>98%, 24 h), while ZW800-1A conjugates degraded rapidly after 4 h (22–62%, 24 h). The hydrolyzed form of cRGD-ZW800-1A was confirmed using HPLC-MS TOF (Figure 4C). These results demonstrate the feasibility of using C-C bonded structures to label bioactive molecules because of their enhanced optical and chemical stability after conjugation in terms of the biological applications.

In summary, we designed C-C coupled ZW800 analogs to improve the photostability of oxygen-substituted ZW800 compounds in biological and physiological conditions. Both ZW800-1C and ZW800-3C have highly stable chemical and optical properties *in vitro* and *in vivo*. Moreover, the reactive carboxylate moiety on the stable *meso* carbon allows further modification of the contrast agent for conjugation with targeting ligands including small molecules, peptides, and proteins for various biomedical applications.

Online Methods

Synthesis of C-C coupled ZW800 analogs

The chemical reagents used in the synthesis of all compounds were obtained from Sigma-Aldrich (Saint Louis, MO) and Alfa Aesar (Ward Hill, MA). All compounds were purified by column chromatography and obtained in high purity as indicated by TLC analyses using C18 adsorbents and high-resolution ^{1}H and ^{13}C NMR spectra (Bruker Avance, 400 MHz). Chemical purity was also confirmed using high-resolution accurate mass spectra (HRMS) equipped with a Waters Q-TOF micro (ESI-Q-TOF) mass spectrometer. See Supplementary Information for detailed chemical syntheses and analyses.

Conjugation with biomolecules

N-Hydroxysuccinimide (NHS) activated ZW800-1A and ZW800-1C were conjugated to Cyclo(Arg-Gly-Asp-D-Tyr-Lys) peptide (cRGDyK; MW 619.6, AnaSpec), bovine serum albumin (BSA; MW 67 kDa, Sigma-Aldrich), mouse IgG (IgG; MW 150 kDa, Sigma-Aldrich), and poly-ε-lysine (MW 4 kDa, Chisso Corp, Yokohama, Japan), respectively. cRGD-ZW800 conjugates were separated by preparative HPLC system (Waters, Milford, MA, USA) equipped with a PrepLC 150 mL fluid handling unit, a manual injector (Rheodyne 7725i), a 2487 dual wavelength absorbance detector (Waters) and an evaporative light scatter detection (ELSD, Richards Scientific, Novato, CA, USA). BSA-, IgG-, and poly-ε-lysine-ZW800 conjugates were purified by gel-filtration chromatography (GFC) using Bio-Scale Mini Bio-Gel P-6 Desalting columns (Bio-Rad). The labeling ratio was calculated from the ratio of extinction coefficients between the BSA, antibody, and ZW800 fluorophores. See Figure S5 in Supplementary Information for detailed analyses.

Stock solution preparation

The stock solution of each fluorophore was prepared by weighing the solid on a 5-digit analytical balance directly into a brown vial and dissolving the appropriate masses in dimethyl sulfoxide (DMSO) to the final concentration to be 10 mM. The contents of the vial were vortexed for 30 sec, then sonicated for 10 min to ensure complete dissolution. The

working solutions were prepared by diluting the each stock solution to the final concentration of 100 μM in the solvents of interest. The sample dilutions were subsequently prepared immediately prior to use by the dilution of the working stock solutions to final concentrations with the solvents of interest. For the PBS studies the dilutions contained a 98% PBS and 2% DMSO. All stock solutions were stored in the dark at 4 °C when not in use.

Optical property measurements

All optical measurements were performed at 37 °C in PBS, pH 7.4 or 100% FBS buffered with 50 mM HEPES, pH 7.4. For measuring fluorescence spectra of targeted NIR fluorophores, NIR excitation was provided by a 770 nm NIR laser diode light source (Electro Optical Components, Santa Rosa, CA) set to 10 mW and coupled through a 300 μm core diameter, NA 0.22 fiber (Fiberguide Industries, Stirling, NJ).[23] *In silico* calculations of the partition coefficient (logD at pH 7.4) and surface molecular charge and hydrophobicity were calculated using MarvinSketch 5.2.1 by taking major microspecies at pH 7.4 (ChemAxon, Budapest, Hungary).

Intraoperative NIR fluorescence imaging system

The dual-NIR channel FLARE™ imaging system has been described in detail previously.[24,25] In this study, a 760 nm excitation fluence rate used was a 11.0 mW/cm^2 with white light (400 to 650 nm) at 40,000 lx. Color video and NIR fluorescence images were acquired simultaneously with custom FLARE software at rates up to 15 Hz over a 15 cm diameter field of view (FOV). The imaging system was positioned at a distance of 18 inches from the surgical field. A custom filter set (Chroma Technology Corporation, Brattleboro, VT) composed of a 750 ± 25 nm excitation filter, a 785 nm dichroic mirror, and an 810 ± 20 nm emission filter were used.

In vivo biodistribution and clearance

Animals were housed in an AAALAC-certified facility and were studied under the supervision of BIDMC IACUC in accordance with approved institutional protocols (#101-2011 for rodents and #046-2010 for pigs). Male CD-1 mice weighing ≈25 g and male Sprague-Dawley (SD) rats weighing ≈250 g (Charles River Laboratories, Wilmington, MA) were anesthetized with 100 mg/kg ketamine and 10 mg/kg xylazine intraperitoneally (Webster Veterinary, Fort Devens, MA). Female Yorkshire pigs (E.M. Parsons and Sons, Hadley, MA) averaging 35 kg were induced with 4.4 mg/kg intramuscular Telazol™ (Fort Dodge Labs, Fort Dodge, IA), intubated, and maintained with 2% isoflurane (Baxter Healthcare Corp., Deerfield, IL). Following anesthesia, electrocardiogram, heart rate, pulse oximetry, and body temperature were monitored throughout surgery. At each time point, the fluorescence (FL) and background (BG) intensity of a region of interest (ROI) over each organ/tissue was quantified using custom FLARE software. The signal-to-background ratio (SBR) of each organ was calculated against surrounding muscle using ImageJ version 1.45q. All NIR fluorescence images for a particular fluorophore were normalized identically for all conditions of an experiment. At least 3 animals were analyzed at each time point. Results

were presented as mean ± s.d. and curve fitting was performed using Prism version 4.0a software (GraphPad, San Diego, CA).

Supplementary Material

Refer to Web version on PubMed Central for supplementary material.

Acknowledgments

We thank David Burrington, Jr. for editing and Eugenia Trabucchi for administrative assistance. This study was supported by the following grants from the National Institutes of Health: NCI BRP grant #R01-CA-115296 (JVF), NIBIB grant #R01-EB-010022 (JVF), and NIBIB grant #R01-EB-011523 (HSC).

References

1. Tao HQ, Yang K, Ma Z, Wan JM, Zhang YJ, Kang ZH, Liu Z. Small. 2012; 8:281–290. [PubMed: 22095931]
2. Collado D, Vida Y, Najera F, Perez-Inestrosa E. Rsc Advances. 2014; 4:2306–2309.
3. Yue CX, Liu P, Zheng MB, Zhao PF, Wang YQ, Ma YF, Cai LT. Biomaterials. 2013; 34:6853–6861. [PubMed: 23777910]
4. Luo SL, Zhang EL, Su YP, Cheng TM, Shi CM. Biomaterials. 2011; 32:7127–7138. [PubMed: 21724249]
5. Owens EA, Hyun H, Kim SH, Lee JH, Park G, Ashitate Y, Choi J, Hong GH, Alyabyev S, Lee SJ, Khang G, Henary M, Choi HS. Biomed Mater. 2013; 8:014109. [PubMed: 23353870]
6. Henary M, Pannu V, Owens EA, Aneja R. Bioorganic & Medicinal Chemistry Letters. 2012; 22:1242–1246. [PubMed: 22177785]
7. Choi HS, Nasr K, Alyabyev S, Feith D, Lee JH, Kim SH, Ashitate Y, Hyun H, Patonay G, Strekowski L, Henary M, Frangioni JV. Angew Chem Int Ed Engl. 2011; 50:6258–6263. [PubMed: 21656624]
8. Choi HS, Gibbs SL, Lee JH, Kim SH, Ashitate Y, Liu F, Hyun H, Park G, Xie Y, Bae S, Henary M, Frangioni JV. Nat Biotechnol. 2013; 31:148–153. [PubMed: 23292608]
9. Hyun H, Bordo MW, Nasr K, Feith D, Lee JH, Kim SH, Ashitate Y, Moffitt LA, Rosenberg M, Henary M, Choi HS, Frangioni JV. Contrast Media Mol Imaging. 2012; 7:516–524. [PubMed: 22991318]
10. Zhang S, Fan JL, Li ZY, Hao NJ, Cao JF, Wu T, Wang JY, Peng XJ. Journal of Materials Chemistry B. 2014; 2:2688–2693.
11. Xin J, Zhang XH, Liang JM, Xia LM, Yin JP, Nie YZ, Wu KC, Tian J. Bioconjugate Chemistry. 2013; 24:1134–1143. [PubMed: 23725355]
12. Yu FB, Li P, Song P, Wang BS, Zhao JZ, Han KL. Chemical communications. 2012; 48:4980–4982. [PubMed: 22499337]
13. Yang XJ, Shi CM, Tong R, Qian WP, Zhau HE, Wang RX, Zhu GD, Cheng JJ, Yang VW, Cheng TM, Henary M, Strekowski L, Chung LWK. Clinical Cancer Research. 2010; 16:2833–2844. [PubMed: 20410058]
14. Miletto I, Gilardino A, Zamburlin P, Dalmazzo S, Lovisolo D, Caputo G, Viscardi G, Martra G. Dyes and Pigments. 2010; 84:121–127.
15. Pandey RK, James N, Chen YH, Dobhal MP. Heterocyclic Polymethine Dyes. 2008; 14:41–74.
16. Carreon JR, Stewart KM, Mahon KP, Shin S, Kelley SO. Bioorganic & Medicinal Chemistry Letters. 2007; 17:5182–5185. [PubMed: 17646099]
17. Yang CM, Shimelis O, Zhou XJ, Li GD, Bayle C, Nertz M, Lee H, Strekowski L, Patonay G, Couderc F, Giese RW. Journal of Chromatography A. 2002; 979:307–314. [PubMed: 12498262]
18. Gai W, Yang QF, Xiang JF, Jiang W, Li Q, Sun HX, Guan AJ, Shang Q, Zhang H, Tang YL. Nucleic acids research. 2013; 41:2709–2722. [PubMed: 23275573]

19. Nanjunda R, Owens EA, Mickelson L, Alyabyev S, Kilpatrick N, Wang SM, Henary M, Wilson WD. Bioorganic & Medicinal Chemistry. 2012; 20:7002–7011. [PubMed: 23127491]

20. Yang QF, Xiang JF, Yang S, Zhou QJ, Li Q, Tang YL, Xu GZ. Chemical communications. 2009:1103–1105. [PubMed: 19225650]

21. Lee H, Mason JC, Achilefu S. J Org Chem. 2006; 71:7862–7865. [PubMed: 16995699]

22. Abd El-Aal RM, Younis M. Bioorg Chem. 2004; 32:193–210. [PubMed: 15210335]

23. Ashitate Y, Hyun H, Kim SH, Lee JH, Henary M, Frangioni JV, Choi HS. Theranostics. 2014; 4:693–700. [PubMed: 24883119]

24. Choi HS, Frangioni JV. Molecular imaging. 2010; 9:291–310. [PubMed: 21084027]

25. Choi HS, Ashitate Y, Lee JH, Kim SH, Matsui A, Insin N, Bawendi MG, Semmler-Behnke M, Frangioni JV, Tsuda A. Nature biotechnology. 2010; 28:1300–1303.

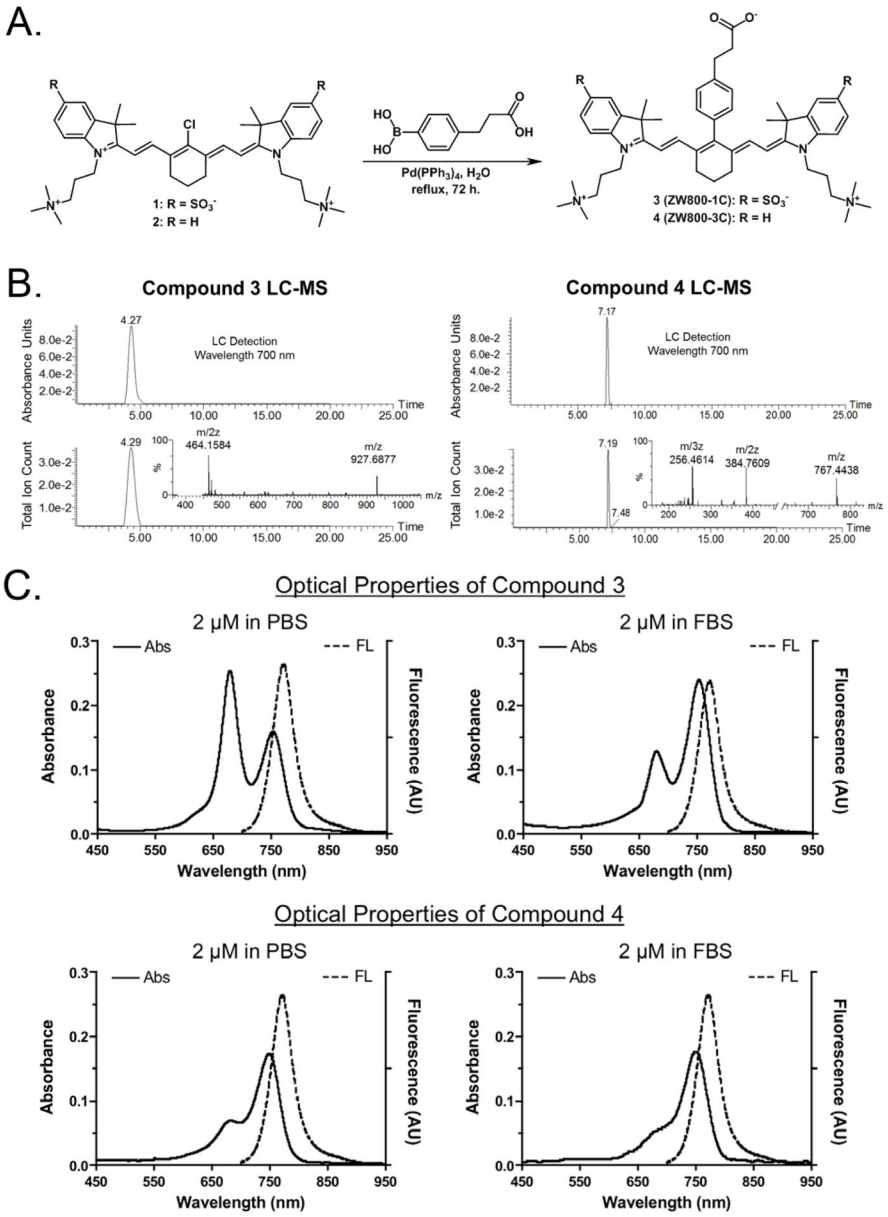

D. Optical Properties of ZW800-1C and ZW800-3C in Various Solvents.

Fluorophore	Solvent	λ_{max}^{Abs} (nm)	λ_{max}^{Em} (nm)	SS (nm)	ε ($M^{-1}cm^{-1}$)	R^2
3: ZW800-1C	MeOH	762	781	19	82,000	0.992
	DMSO	779	798	19	125,000	0.998
	PBS	753 (m) / 678 (d)	772	19	123,000	0.999
	FBS	754 (m) / 680 (d)	776	22	111,000	0.996
4: ZW800-3C	MeOH	753	773	20	82,000	0.992
	DMSO	769	788	19	171,000	0.997
	PBS	748 (m) / 678 (d)	768	20	76,000	0.992
	FBS	749	769	20	87,000	0.995

MeOH = methanol; DMSO = dimethyl sulfoxide; PBS = phosphate buffered saline, pH 7.4; FBS = fetal bovine serum supplemented with 50 mM HEPES, pH 7.4; λ_{max}^{Abs} = peak absorption wavelength; λ_{max}^{Em} = peak emission wavelength; SS = Stokes shift; m = monomer; d = dimer.

E. Molecular Brightness in 100% FBS supplemented with 50 mM HEPES, pH 7.4.

Property in FBS	ZW800-1C	ZW800-1	ZW800-3C	ZW800-3
ε ($M^{-1}cm^{-1}$)	111,000	249,000	87,000	309,000
QY (%)	23.9	15.1	19.2	16.1
Molecular Brightness	26,529	37,599	16,704	49,749

Figure 1. Chemical syntheses and optical properties of 3 (ZW800-1C) and 4 (ZW800-3C)

(**a**) Synthesis of compounds **3** and **4** by the Suzuki-coupling using palladium catalyst in water. (**b**) LC-MS analysis and purity (%) of C-C coupled compounds: absorbance at 700 nm (top) and total ion chromatogram (TIC, bottom), and ESI-TOF mass spectrum (inserted). (**c**) Absorbance and fluorescence spectra of fluorophores **3** and **4** measured in PBS (pH 7.4) and FBS (supplemented with 50 mM HEPES, pH 7.4). (**d**) Optical properties of fluorophores **3** and **4** in various solvents (**e**) Molecular Brightness in 100% FBS supplemented with 50 mM HEPES, pH 7.4.

A.

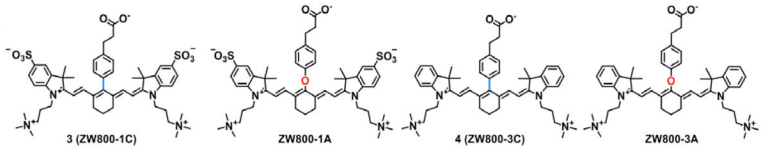

Physicochemical Property	3: ZW800-1C	ZW800-1A[8]	4: ZW800-3C	ZW800-3A[8]
Charges (+/-)	+3 / -3	+3 / -3	+3 / -1	+3 / -1
LogD, pH 7.4	-2.80	-3.35	-1.25	-1.63
Acidic / Basic pKa	-3.59 / 0.51	-3.59 / 0.50	4.21 / 1.70	4.04 / 1.69
Rotatable Bonds	17	18	15	16
H-Bond Acceptor / Donor	9 / 1	10 / 1	3 / 1	4 / 1
Polar Surface Area (Å^2)	157.95	167.18	43.55	52.78

B. Photostability in 100% FBS supplemented with 50 mM HEPES, pH 7.4.

Incubation Time	3: ZW800-1C	ZW800-1A	4: ZW800-3C	ZW800-3A
0 h	100%	100%	100%	100%
4 h	100%	95.6%[8]	99.6%	96.2%[8]
24 h	99.8%	52.9%	99.5%	55.8%

Figure 2. Physicochemical and optical stabilities of 3 (ZW800-1C) and 4 (ZW800-3C)

(**a**) Molecular structures and physicochemical properties of C-C coupled fluorophores ZW800-1C and ZW800-3C compared to oxygen-substituted ZW800-1A and ZW800-3A. (**b**) Time-dependent optical stability of each fluorophore in 100% FBS supplemented with 50 mM HEPES, pH 7.4.

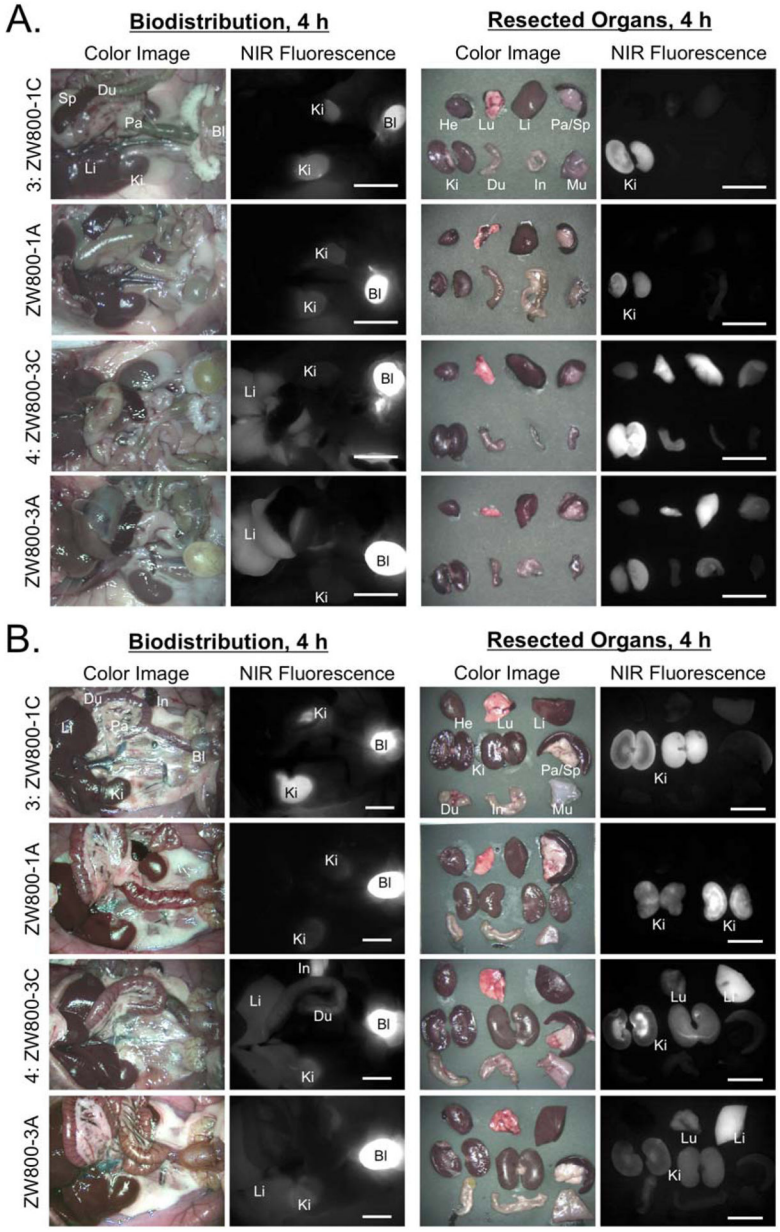

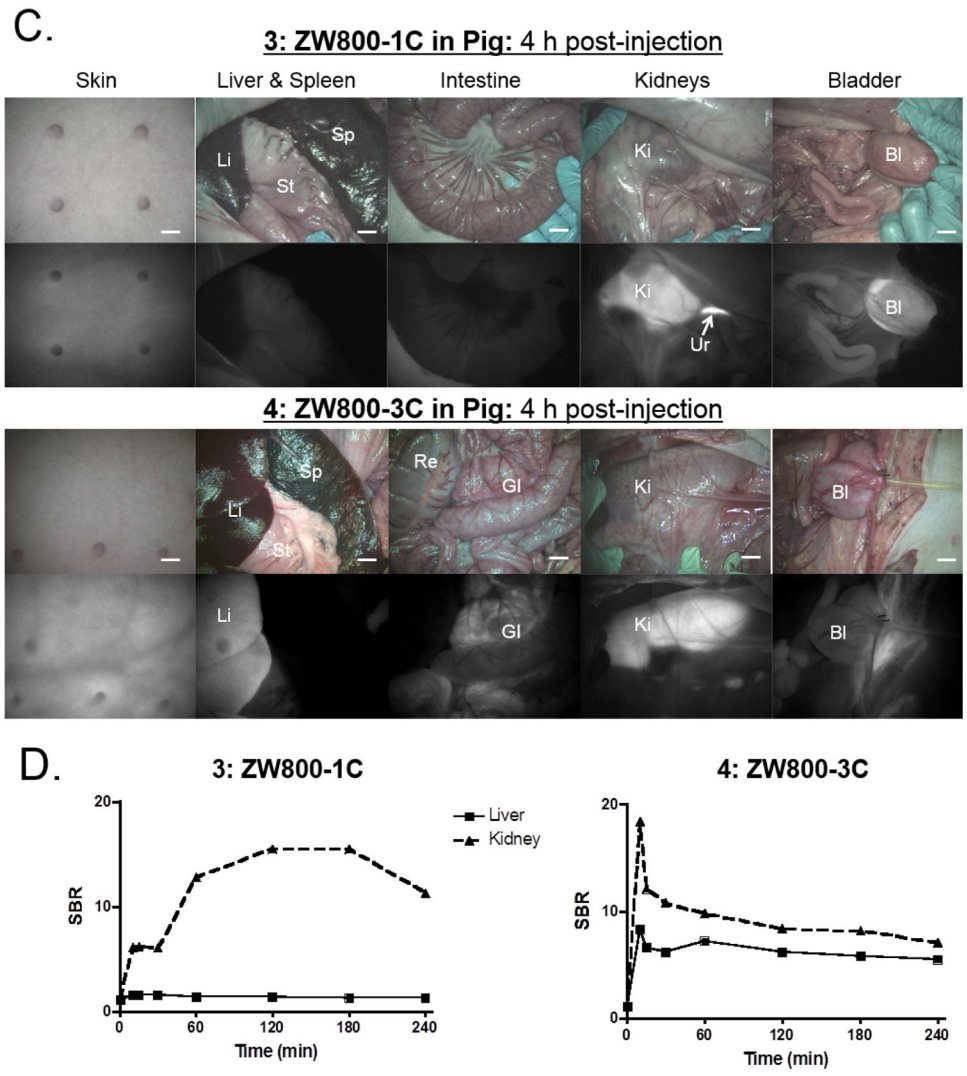

Figure 3. Biodistribution and clearance of ZW800-1C and ZW800-3C

Each compound was injected intravenously into CD-1 mice (**a**, 25 nmol), SD rats (**b**, 100 nmol), and Yorkshire pigs (**c**, 5 μmol) 4 h prior to imaging. Scale bars = 1 cm. (**d**) Signal-to-background ratio (SBR) in kidneys and liver against surrounding muscle was observed up to 4 h post-injection measured in pigs. Abbreviations used are: Bl, bladder; Du, duodenum; GI, gastrointestinal track; He, heart; In, intestine; Ki, kidneys; Li, liver; Lu, lungs; Mu, muscle; Pa, pancreas; Re, rectum; Sp, spleen; St, stomach and Ur, ureter.

A.

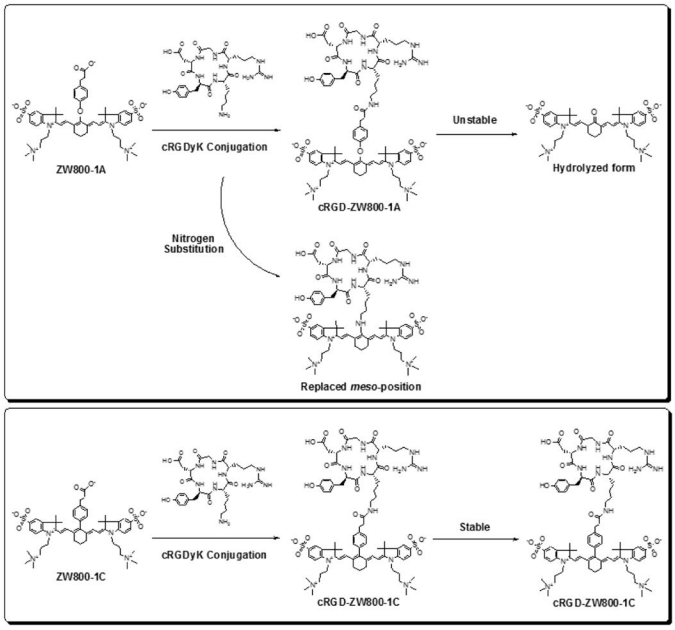

B. Photostability of ZW800-1C and ZW800-1A conjugates in 100% serum for 4 h and 24 h.

Compound	cRGDyK		BSA		IgG		Poly-ε-lysine	
Incubation time	4 h	24 h	4 h	24h	4 h	24h	4 h	24h
ZW800-1A	93%	34%	94%	62%	78%	56%	84%	22%
ZW800-1C	100%	98%	100%	99%	100%	99%	100%	98%

C.

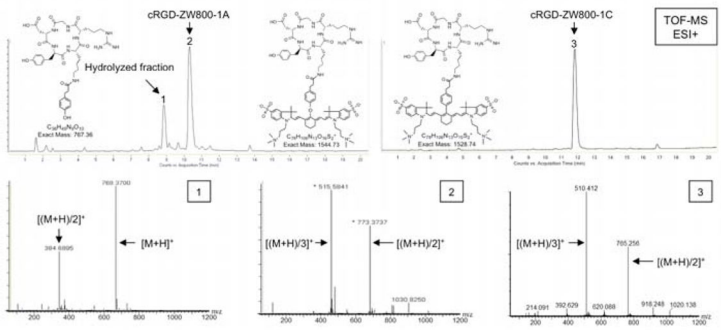

Figure 4. Chemical conjugation of cRGDyK with ZW800-1A and ZW800-1C

(**a**) Conjugation schemes of cRGD-ZW800-1A and cRGD-ZW800-1C and possible byproducts. (**b**) Photostability of ZW800-1A and ZW800-1C conjugates in 100% serum for 4 h and 24 h. (**c**) HPLC-MS analysis of cRGD-ZW800-1A and cRGD-ZW800-1C after 24 h incubation in 100% FBS supplemented with 50 mM HEPES, pH 7.4.